

QCD corrections to non-standard WZ+jet production with leptonic decays at the LHC

Francisco Campanario*

Institute for Theoretical Physics, KIT, 76128 Karlsruhe, Germany

Christoph Englert†

*Institute for Theoretical Physics, KIT, 76128 Karlsruhe, Germany and
Institute for Theoretical Physics, Heidelberg University, 69120 Heidelberg, Germany*

Michael Spannowsky‡

Institute for Theoretical Science, University of Oregon, Eugene Oregon 97403, USA

We discuss the impact of anomalous $WW\gamma$ and WWZ couplings on WZ+jet production at next-to-leading order QCD, including full leptonic decays of the electroweak gauge bosons. While the inclusive hadronic cross sections do not exhibit any particular sensitivity to anomalous couplings once the residual QCD scale uncertainties are taken into account, the transverse momentum distributions show substantial deviations from the Standard Model, provided that the anomalous vertices are probed at large enough momentum transfers.

PACS numbers: 12.38.Bx, 12.60.Cn, 13.85.-t

I. INTRODUCTION

Searches for anomalous trilinear electroweak couplings at hadron colliders is an active field of research to discover new interactions beyond the well-established Standard Model of particle physics (SM), see, e.g., [1] for very recent $D\emptyset$ results. Crucial for revealing modifications of the electroweak sector is, without any doubt, adequate experimental and theoretical precision of measurement and simulation, respectively. Since corrections from Quantum chromodynamics (QCD) are typically sizable at hadron colliders, they have to be properly included in phenomenological studies in order not to misinterpret QCD dynamics for beyond-the-SM (BSM) interactions when data is analyzed. Hence, an important step towards resolving these QCD-related issues is studying important production processes at least to next-to-leading order (NLO) QCD precision.

The NLO QCD corrections to anomalous WZ and $W\gamma$ production have already been discussed in the literature in detail, e.g. in Refs. [2, 3]. At the LHC, with its large center-of-mass energy of expected 14 TeV, additional jet radiation from accessing gluon-induced channels with large parton luminosities is substantially important for these processes, which are exclusively quark-induced at LO. Moreover, the additional parton emission represents a theoretically indispensable real emission contribution to the infrared-safe NLO QCD diboson cross section via the Kinoshita-Lee-Nauenberg theorem [4]. By probing the gluon-induced channels at small momentum

fractions with respect to the incoming protons, the one-jet-contribution becomes comparable to the leading order (zero jet) cross section for typical selection criteria*,

$$\frac{\sigma(pp \rightarrow 3 \text{ leptons} + \cancel{p}_T + \text{jet})}{\sigma(pp \rightarrow 3 \text{ leptons} + \cancel{p}_T)} \simeq 1. \quad (1)$$

Hence, for inclusive measurements, the perturbative uncertainty of NLO WZ production is heavily affected by the one jet contribution, which is leading order (LO) in the strong coupling-expansion.

Since the gluon-induced real emission contributions kinematically obstruct anomalous coupling measurements, one often reverts to jet vetos, at least in some way, when performing phenomenological studies, e.g. in Ref. [3]. Hence, considering exclusive NLO production [2], one is able to increase the sensitivity of the WZ cross section to anomalous couplings, which we define to be $\sigma(\text{non-SM})/\sigma(\text{SM})$ in the following. From a perturbative QCD point of view, however, this strategy does not necessarily give rise to improved QCD precision of total cross sections, even if improved renormalization and factorization scale dependencies might superficially suggest so. To arrive at seemingly stable NLO results, one subtracts a dominant and unreliable $\text{LO-}\alpha_s$ contribution. Since this very contribution is sensitive to the applied hadronic cuts, one is able, given a relation analogous to Eq. (1), to tune the real emission contribution to milden the factorization and renormalization scale dependencies at the integrated cross section level †. This

*Electronic address: francam@particle.uni-karlsruhe.de

†Electronic address: c.englert@thphys.uni-heidelberg.de

‡Electronic address: mspannow@uoregon.edu

*We refer to the considered processes $pp \rightarrow \ell^- \bar{\nu}_\ell \ell'^+ \ell'^- + \text{jet}$ and $pp \rightarrow \ell^+ \nu_\ell \ell'^+ \ell'^- + \text{jet}$, where ℓ, ℓ' denote light but distinct lepton flavors, as $W^\pm Z + \text{jet}$ production in this paper.

†Indeed, this is the case for e.g. $W\gamma + \text{jet}$ production, where a more

signalizes the necessity to also take into account the differential QCD corrections to diboson production in association with a hard jet, to add NLO precision to the veto performance. The quantitative dependence of the QCD corrections on the anomalous couplings in this context supplements the necessary additional information to recent theoretical leading order analysis [5].

Eq. (1) also raises the question whether there is enough sensitivity to anomalous couplings left at larger inclusive rates, which could supplement the powerful “traditional” measurement strategies, that exploit the well-known classical radiation zeros in the $q\bar{Q} \rightarrow W\gamma, WZ$ amplitudes in the SM [6]. Given Eq. (1), the sensitivity to anomalous couplings in inclusive phenomenological analysis crucially depends on the one jet-inclusive cross section. A reliable assessment of the anomalous couplings’ impact is then only possible if QCD corrections are properly included as they have turned out to be particularly sizable for the diboson+jet cross sections in Refs. [7–10].

To contribute to resolving the above issues, we report in this paper on the calculation of non-standard WZ +jet production at NLO QCD. We compute the WZ +jet cross sections and distributions as functions of the anomalous couplings’ parameters by means of a fully-flexible Monte Carlo program that has been designed for the purpose of this work. Full leptonic decays of the W and Z bosons are included throughout. The code will be publicly available with an upcoming update of VBFNLO [11], and is also capable of performing Tevatron calculations. We give details on the computation in Sec. II, and Sec. III is devoted to the numerical results. In particular, we compare the impact of anomalous couplings to the scale uncertainty of the SM cross section for inclusive selection cuts and for a cut choice that mimics genuine WZ events. For the latter, we discuss the anomalous couplings’ impact on the differential cross sections in more detail. Sec. IV closes with a summary of this work.

II. DETAILS OF THE CALCULATION

The strategy and the methods we apply to perform the NLO calculation in a fast and numerically stable way have already been presented in detail in Refs. [8, 10]. We therefore only sketch the numerical implementation to make this work self-consistent. To arrive at the numerical results of Sec. III, we use a modified version of the Monte Carlo code of Ref. [10], which builds upon the VBFNLO framework [11]. We evaluate the LO matrix elements for $pp \rightarrow 3 \text{ leptons} + \cancel{p}_T + \text{jet}$ at $\mathcal{O}(\alpha_s\alpha^4)$ via HELAS routines [12], which are set up with MADGRAPH [13]. The virtual and real emission matrix elements are computed

numerically using in-house routines along the lines described in Refs. [8, 10]. Algebraic bookkeeping of the infrared singularities is thereby performed by applying the method of Catani and Seymour [14]. Throughout the computation, the anomalous trilinear couplings are included via purpose-built HELAS routines, which we design using an in-house framework that employs FEYN-RULES [15]. The anomalous trilinear vertices follow from the most general Lorentz-, \mathcal{CP} -, and QED-invariant effective operators up to dimension six [2, 16],

$$\begin{aligned} \mathcal{L}_{WW\gamma} = & -ie [W_{\mu\nu}^\dagger W^\mu A^\nu - W_\mu^\dagger A_\nu W^{\mu\nu} \\ & + \kappa_\gamma W_\mu^\dagger W_\nu F^{\mu\nu} + \frac{\lambda_\gamma}{m_W^2} W_{\lambda\mu}^\dagger W_\nu^\mu F^{\nu\lambda}] \end{aligned} \quad (2)$$

for the anomalous $WW\gamma$ vertex, and

$$\begin{aligned} \mathcal{L}_{WWZ} = & -ie \cot \theta_w [g_1^Z (W_{\mu\nu}^\dagger W^\mu A^\nu - W_\mu^\dagger A_\nu W^{\mu\nu}) \\ & + \kappa_Z W_\mu^\dagger W_\nu Z^{\mu\nu} + \frac{\lambda_Z}{m_W^2} W_{\lambda\mu}^\dagger W_\nu^\mu Z^{\nu\lambda}] \end{aligned} \quad (3)$$

for the anomalous WWZ vertex. In Eq. (3) θ_w denotes the weak mixing angle. W^μ , A^μ , and Z^μ denote the W , the photon and the Z boson. The field strength tensors are $F^{\mu\nu} = \partial^\mu A^\nu - \partial^\nu A^\mu$, $Z^{\mu\nu} = \partial^\mu Z^\nu - \partial^\nu Z^\mu$, and $W^{\mu\nu} = \partial^\mu W^\nu - \partial^\nu W^\mu$, as usual. We do not include \mathcal{CP} -violating operators since they are already heavily constrained by measurements of the neutron’s electric dipole moment (Ref. [2, 17]). We thus can focus on the W^-Z +jet production for brevity, and our findings generalize to W^+Z +jet production in a rather straightforward fashion. The W^+Z +jet cross sections are, however, larger by a factor 1.5 due to testing the protons’ valence quarks.

We apply the gauge constraints, which were used for the combined analysis of LEP data in Ref. [18],

$$\kappa_Z = g_1^Z - (\kappa_\gamma - 1) \tan^2 \theta_w, \quad \lambda_Z = \lambda_\gamma. \quad (4)$$

This analysis also gives rise to the currently most stringent bounds on anomalous trilinear couplings,

$$\begin{aligned} g_1^Z = & 0.991_{-0.021}^{+0.022}, \quad \kappa_\gamma = 0.984_{-0.047}^{+0.042}, \\ \lambda_\gamma = & -0.016_{-0.023}^{+0.021}, \end{aligned} \quad (5)$$

at 68% confidence level. Most constraining bounds at hadron colliders have only recently been obtained from direct measurements of the WWZ vertex at the Fermilab $D\bar{O}$ [1].

Unitarity requires the anomalous parameters $\{g_1^Z, \kappa_Z, \lambda_Z, \kappa_\gamma, \lambda_\gamma\}$ to be understood as low-energy form factors. Their precise momentum dependence is determined by the BSM Lagrangian. Avoiding any particular assumption about how the BSM interactions might look like (except for participation in SM interactions of some kind), we use the conventional dipole parametrization of the form factors, Ref. [2]. Introducing

thorough investigation reveals sophisticated cancellations of scale dependencies for the NLO exclusive cross sections, rendering the perturbative stability unreliable.

new parameters, which rephrase the modifications of Eqs. (2) and (3) around the SM Lagrangian,

$$(\Delta g_1^Z, \Delta \kappa_Z, \Delta \kappa_\gamma) = (g_1^Z, \kappa_Z, \kappa_\gamma) - 1, \quad (6)$$

the dipole profile is given by

$$(\Delta g_1^Z, \Delta \kappa_Z, \lambda_Z, \Delta \kappa_\gamma, \lambda_\gamma) = \frac{(\Delta g_1^{Z,0}, \Delta \kappa_Z^0, \lambda_Z^0, \Delta \kappa_\gamma^0, \lambda_\gamma^0)}{(1 + m_{WZ}^2/\Lambda^2)^2}, \quad (7)$$

where m_{WZ} denotes the invariant mass of the decaying WZ or $W\gamma$ pair, and Λ is the scale where new physics enters the picture. The momentum dependence of Eq. (7) guarantees vanishing contributions from phase space regions where the naive momentum-independent parametrization violates unitarity. In addition, given the steeply falling parton luminosities for large parton momentum fractions, a well-behaved theory yields vanishing contributions in this particular region, so that the parametrization of Eq. (7) is adequate for phenomenological studies. In the following, we choose $\Lambda = 2$ TeV, which is also a benchmark point of various experimental studies (e.g. in Ref. [1, 3]).

III. NUMERICAL RESULTS

For the numerical results, we use CTEQ6M parton distributions [19] and the CTEQ6L1 set at LO. We choose $m_Z = 91.188$ GeV, $m_W = 80.419$ GeV and $G_F = 1.16639 \times 10^{-5}$ GeV⁻² as electroweak input parameters and derive the electromagnetic coupling α and the weak mixing angle from Standard Model-tree level relations. The LO and NLO running of the strong coupling α_s is determined by $\alpha_s^{\text{LO}}(m_Z) = 0.130$ and $\alpha_s^{\text{NLO}}(m_Z) = 0.118$ with five active flavors, respectively. We fix the center-of-mass energy to 14 TeV for LHC collisions, and we sum

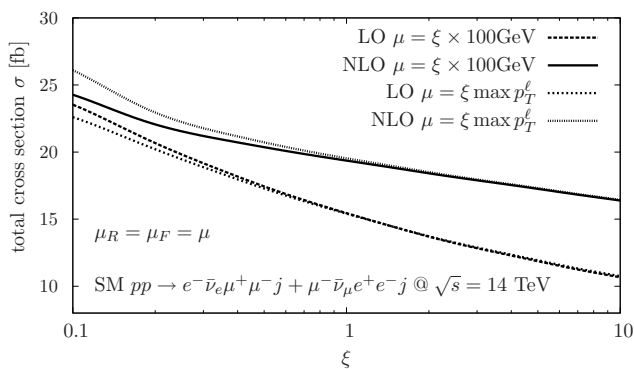


FIG. 1: Scale dependence of the SM cross section at LO and NLO for the set up described in Sec. III. In addition to the fixed-scale variation, we also plot the variation for renormalization and factorization scales chosen to be the maximum transverse momentum of the charged leptons. Varying μ by a factor two around $\xi = 1$ reduces the uncertainties from 24% (23%) at LO to 9% (10%) at NLO for $\mu = \xi \times 100$ GeV ($\mu = \xi \max p_T^l$).

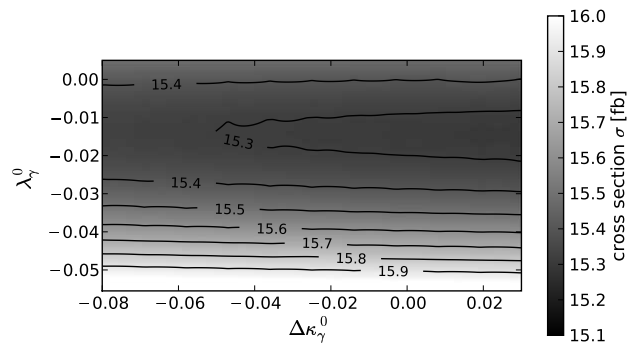


FIG. 2: Total LO cross section contours in fb for $W^- Z + \text{jet}$ production for the cut and parameter choices as described in the text. We use a fixed-scale choice $\mu_R = \mu_F = 100$ GeV. Additionally, we choose $\Delta g_1^{Z,0} = 0$.

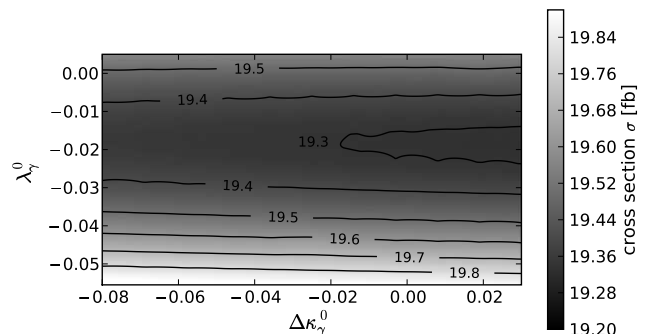


FIG. 3: Total NLO cross section contours in fb for $W^- Z + \text{jet}$ production analogous to Fig. 2.

over the light lepton flavors in the final state, which we treat as massless.

Additionally, we neglect processes subject to Pauli-interference, i.e. we quote results for $pp \rightarrow e^- \bar{\nu}_e \mu^+ \mu^- j + X$ plus $pp \rightarrow \mu^- \bar{\nu}_\mu e^+ e^- j + X$ in case of $W^- Z + \text{jet}$ production[‡]. Lowering the available LHC energy to 7 TeV yields a too low rate to be of phenomenological importance given the scheduled integrated luminosity of 1 fb⁻¹. Since anomalous couplings alter the high-energy phenomenology, $WZ + \text{jet}$ production from Tevatron collisions does not yield any notable sensitivity in the allowed parameter range.

The CKM matrix is assumed to be diagonal, which is an excellent approximation for LHC cross sections [10]. Jets are recombined via the algorithm of [20] from partons which fall in the pseudorapidity range of $|\eta| \leq 5$. The jet resolution parameter is chosen to be $D = 0.7$,

[‡]Since Pauli-interference is a small effect for our process, we could as well multiply our results for the total cross section and differential distributions by a global factor 1.5 to account for the processes with identical final state lepton flavors.

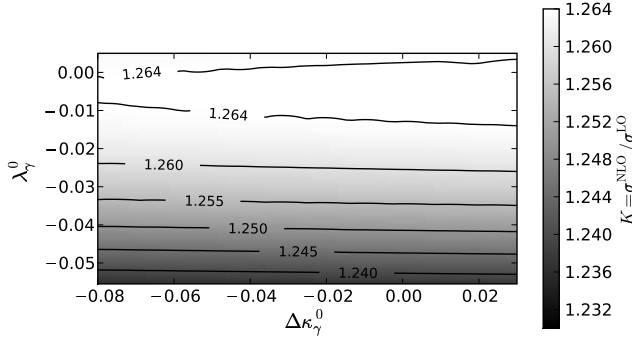


FIG. 4: Total K factor contours for W^-Z + jet production analogous to Fig. 2.

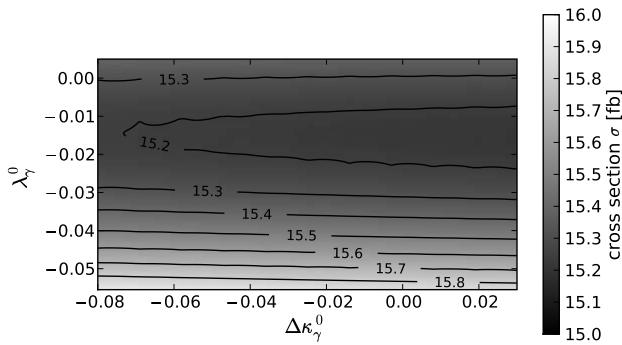


FIG. 5: Total NLO cross section contours in fb for W^-Z + jet production for the cut and parameter choices as described in the text, with the additional requirement of Eq. (13). We again choose $\Delta g_1^{Z,0} = 0$. We choose $\mu_R = \mu_F = \max p_T^\ell$.

and the jets are required to lie in the rapidity range accessible to the detector

$$|y_j| \leq 4.5. \quad (8)$$

For the charged leptons, we request

$$|\eta_\ell| \leq 2.5. \quad (9)$$

We choose a very inclusive cut set-up in order to analyze the anomalous couplings' impact on the phenomenology of WZ + jet production over a wide range of accessible phase space at the LHC. We require

$$p_T^j \geq 30 \text{ GeV}, \quad p_T^\ell \geq 25 \text{ GeV}, \quad \not{p}_T \geq 25 \text{ GeV}, \quad (10)$$

and, for the jet-lepton and lepton-lepton separation in the azimuthal angle-pseudorapidity plane

$$R_{\ell\ell} = \sqrt{(\Delta\phi_{\ell\ell}^2 + \Delta\eta_{\ell\ell}^2)} \geq 0.2, \quad R_{j\ell} \geq 0.2, \quad (11)$$

for all charged leptons and reconstructed jets.

In Figs. 2 and 3, we representatively scan the NLO cross section for the fixed-scale choice $\mu_R = \mu_F =$

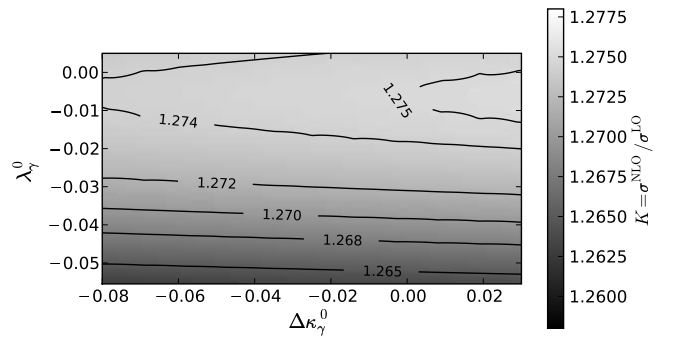


FIG. 6: Total K factor contours for W^-Z + jet production analogous to Fig. 5.

100 GeV over the allowed parameter range for the anomalous couplings of Eq. 5 with the additional requirement $\Delta g_1^{Z,0} = 0$. The total K factor contours,

$$K = \frac{\sigma^{\text{NLO}}}{\sigma^{\text{LO}}}, \quad (12)$$

are depicted in Fig. 4. In particular, the anomalous production cross section mostly depends on the dimension six operators of Eqs. (2) and (3), which are not present in the SM Lagrangian. The QCD corrections are sizable over the whole range of anomalous parameters allowed by LEP measurements. They are especially important for values close to the SM. This follows from the QCD corrections, which turn out to be particularly large around the p_T thresholds and decreasingly important for larger transverse momentum values in the p_T distributions' tails. The corrections for our cut choices are relatively large for small values of $p_T^\ell \lesssim 150$ GeV ($K \simeq 1.3$), where the distributions are unaffected by the anomalous couplings (Fig. 8). The decreasing K factor when approaching the boundaries in Fig. 4 can be understood accordingly: For large values of the anomalous couplings, the cross section is altered already at LO with

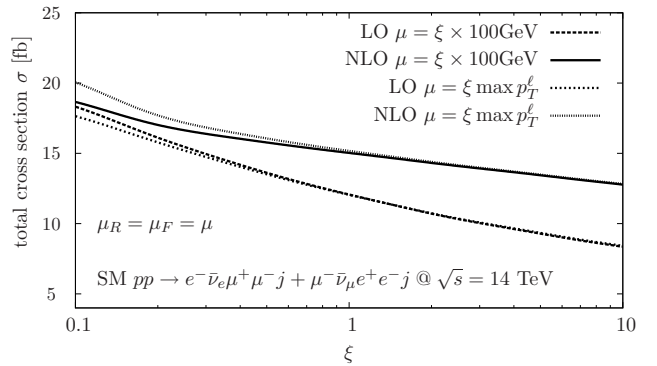


FIG. 7: Scale dependence of the SM cross section at LO and NLO for the inclusive set-up described in Sec. III with the additional requirement of Eq. (13). Analogous to Fig. 1, the scale uncertainty is reduced from 24% (23%) at LO to 10% (11%) at NLO for $\mu = \xi \times 100$ GeV ($\mu = \xi \max p_T^\ell$).

respect to the SM, so that its increase from QCD corrections is less significant. This implies that the NLO QCD corrections decrease the sensitivity to anomalous couplings.

Confronting the non-SM cross sections with the perturbative uncertainty of $\mathcal{O}(10\%)$ for SM-like production, Fig. 1, it is apparent that for our inclusive cuts the impact of the anomalous couplings entirely drowns in the residual QCD scale uncertainty at NLO. In Fig. 1, we also plot the scale variation for the intrinsic scale $\max p_T^\ell$, which is via Eq. (7), related to the characteristic scale of the anomalous couplings. Even for hard events with $\max p_T^\ell \gtrsim 150$ GeV, the impact of the anomalous parameters is not apparent, which also explains the small percent-level deviations of the NLO cross section over the allowed parameter range in Fig. 3. The vanishing sensitivity arises from only small momentum transfers in the anomalous trilinear vertices due to our selection criteria: the jets recoil predominantly against the collinear WZ pair, which is an anomalous couplings-insensitive kinematical configuration. A straightforward way to induce considerably larger momentum transfers while reducing the contributions from anomalous couplings-insensitive graphs, where both the W boson and the Z boson couple to the quark legs, is therefore requiring a large separation of the identically charged decay leptons. Note, that this reflects the kinematics of exclusive diboson production with the W and Z recoiling against each other at LO. A convenient choice is

$$R_{\ell^\pm \ell'^\pm} \geq 1.5. \quad (13)$$

While the cross section decreases by approximately 20%, Fig. 5 reveals cross section deviations due to anomalous couplings of order 5% compared to the SM. Although this is still comparable to the cross section's scale dependence plotted in Fig. 7, its increase compared to the SM entirely results from the large- p_T^ℓ phase space region, Fig. 8. In this region, we find substantial deviations in the $\max p_T^\ell$ shape, which can be well outside the SM scale uncertainty for larger values of the anomalous couplings. Hence, provided a sufficiently large momentum transfer in the anomalous vertices, the WZ +jet production which is vetoed in $pp \rightarrow WZ$ analysis, exhibits potential sensitivity to anomalous couplings via fits to the p_T distributions. However, the total cross section becomes tiny and the sensitivity to anomalous couplings decreases by including the NLO corrections as can be inferred from Figs. 4 and 6.

To this end, it is worthwhile to briefly comment on one-jet exclusive WZ + jet production. In particular, it has been shown that the exclusive diboson+jet cross sections are seemingly stable. In [10], however, it was also shown that applying an additional fixed- p_T jet veto on the second reconstructed jet at NLO yields a poor perturbative reliability. In particular, applying such a veto can lead to negative bins already for modest scales of about 100 GeV. Indeed, this is the phase space region where anomalous couplings give rise to well-pronounced

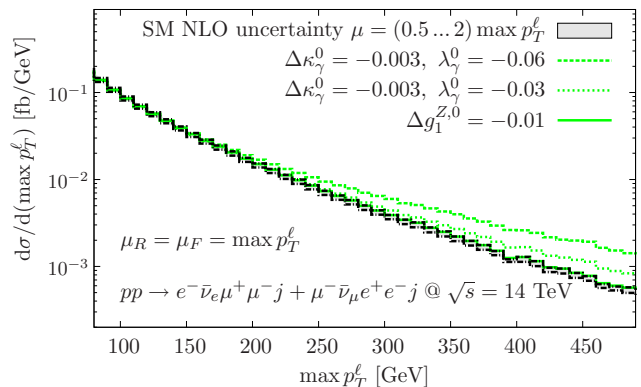


FIG. 8: NLO inclusive distribution of the leptons' maximum transverse momentum $\max p_T^\ell$ for various values of the anomalous couplings. The anomalous parameters which are not quoted are chosen to be zero. The solid line lies within the SM uncertainty band, and the plotted distributions are affected by scale uncertainty bands of equal width. For the shown distributions we have applied the cut of Eq. (13).

deviations from the SM phenomenology (Eq. (7)) at LO. Hence, perturbation theory forces us to consider inclusive production to give reliable predictions at NLO; for our inclusive cut choices with respect to hadronic activity our numerical results are not affected by the mentioned pathologies and can be considered stable except for the residual scale uncertainty of about 10%.

IV. SUMMARY

We have discussed the impact of anomalous trilinear couplings on NLO QCD W^-Z + jet production at the LHC, including leptonic decays. We do not find any significant deviations of differential cross sections, unless we induce sufficiently large momentum transfers in the trilinear vertices. This can be realized by requiring back-to-back WZ pairs. The resulting modifications are characterized by large transverse momenta, and are well-outside the SM scale uncertainty that is intrinsic to our NLO QCD computation for large values of the anomalous couplings in the allowed range by LEP. In general we find that the differential cross sections' sensitivity to anomalous couplings decreases when including inclusive NLO corrections (Figs. 4 and 6), while the QCD corrections do not exhibit any particular dependence on the anomalous parameters. Performing precise measurements in a full hadronic environment, for which our calculation is relevant, requires a careful analysis, taking into account all systematic effects, ranging from showering to detector effects. This is clearly beyond the scope of our calculation. Our Monte Carlo code will be publicly available with an upcoming update of VBFNLO.

Acknowledgments — F.C. acknowledges partial support by FEDER and Spanish MICINN under grant

FPA2008-02878. C.E. and M.S. thank the organizers of the NOBEL (Nordbadische Eliteuniversitäten) particle physics meetings Uli Nierste and Tilman Plehn. C.E. also would like to thank the High Energy Physics group of the Institute for Theoretical Science at the University of Oregon for its hospitality during the time when this

work was completed and acknowledges partial support by “KCETA Strukturiertes Promotionskolleg”. This research is partly funded by the Deutsche Forschungsgemeinschaft under SFB TR-9 “Computergestützte Theoretische Teilchenphysik”, and the Helmholtz alliance “Physics at the Terascale”.

-
- [1] V. Abazov *et al.*, arXiv:1006.0761 [hep-ex].
- [2] U. Baur, T. Han and J. Ohnemus, Phys. Rev. D **48** (1993) 5140, U. Baur, T. Han and J. Ohnemus, Phys. Rev. D **51** (1995) 3381
- [3] M. Dobbs, AIP Conf. Proc. **753**, 181 (2005).
- [4] T. Kinoshita, J. Math. Phys. **3** (1962) 650, T. D. Lee and M. Nauenberg, Phys. Rev. **133** (1964) B1549.
- [5] O. J. P. Eboli, J. Gonzalez-Fraile and M. C. Gonzalez-Garcia, Phys. Lett. B **692** (2010) 20.
- [6] R. W. Brown, K. L. Kowalski and S. J. Brodsky, Phys. Rev. D **28** (1983) 624, U. Baur, T. Han and J. Ohnemus, Phys. Rev. Lett. **72** (1994) 3941.
- [7] S. Dittmaier, S. Kallweit and P. Uwer, Phys. Rev. Lett. **100**, 062003 (2008), J. M. Campbell, R. Keith Ellis and G. Zanderighi, JHEP **0712** (2007) 056, S. Dittmaier, S. Kallweit and P. Uwer, Nucl. Phys. B **826**, 18 (2010).
- [8] F. Campanario, C. Englert, M. Spannowsky and D. Zeppenfeld, Europhys. Lett. **88**, 11001 (2009).
- [9] T. Binoth, T. Gleisberg, S. Karg, N. Kauer and G. Sanguinetti, Phys. Lett. B **683** (2010) 154.
- [10] F. Campanario, C. Englert, S. Kallweit, M. Spannowsky and D. Zeppenfeld, JHEP **1007** (2010) 076.
- [11] K. Arnold *et al.*, Comput. Phys. Commun. **180**, 1661 (2009). The VBFNLO Monte Carlo package can be obtained from <http://www-itp.particle.uni-karlsruhe.de/vbfnlo>.
- [12] H. Murayama, I. Watanabe and K. Hagiwara, KEK-Report 91-11, 1992.
- [13] J. Alwall *et al.*, JHEP **0709** (2007) 028.
- [14] S. Catani and M. H. Seymour, Nucl. Phys. B **485** (1997) 291.
- [15] N. D. Christensen and C. Duhr, Comput. Phys. Commun. **180** (2009) 1614.
- [16] K. Hagiwara, R. D. Peccei, D. Zeppenfeld and K. Hikasa, Nucl. Phys. B **282** (1987) 253.
- [17] C. Amsler *et al.*, Phys. Lett. B **667** (2008) 1.
- [18] J. Alcaraz *et al.*, arXiv:hep-ex/0612034.
- [19] J. Pumplin, D. R. Stump, J. Huston, H. L. Lai, P. Nadolsky, and W. K. Tung, JHEP **0207** (2002), 012.
- [20] S. Catani, Y. L. Dokshitzer, M. H. Seymour, and B. R. Webber, Nucl. Phys. B **406** (1993), 187.